

Clinicopathologic Features of COVID-19: A Case Report and Value of Forensic Autopsy in Studying SARS-CoV-2 Infection

Liang Ren, MD,* Qian Liu, MD,* Rongshuai Wang, MD,† Rong Chen, MD,‡ Qilin Ao, MD,§ Xi Wang, PhD,|| Jie Zhang, PhD,* Fei Deng, PhD,|| Yan Feng, MD,¶ Guoping Wang, MD,§ Yiwu Zhou, MD,* Ling Li, MD,¶ and Liang Liu, MD*

Abstract: As of August 23, 2020, the 2019 novel coronavirus disease (COVID-19) has infected more than 23,518,340 people and caused more than 810,492 deaths worldwide including 4,717 deaths in China. We present a case of a 53-year-old woman who was admitted to the hospital because of dry coughs and high fever on January 26, 2020, in Wuhan, China. She was not tested for SARS-CoV-2 RNA until on hospital day 11 (illness day 21) because of a significant shortage of test kits at the local hospital. Then, her test was positive for COVID-19 on hospital day 20. Despite intensive medical treatments, she developed respiratory failure with secondary bacterial infection and expired on hospital day 23 (3 days after she was tested positive for SARS-CoV-2 RNA). A systemic autopsy examination, including immunohistochemistry and ultrastructural studies, demonstrates that SARS-CoV-2 can infect multiple organs with profound adverse effect on the immune system, and the lung pathology is characterized by diffuse alveolar damage. Extrapulmonary SARS-CoV-2 RNA was detected in several organs postmortem. The detailed pathological features are described. In addition, this report highlights the value of forensic autopsy in studying SARS-CoV-2 infection and the importance of clinicopathological correlation in better understanding the pathogenesis of COVID-19.

Key Words: COVID-19, SARS-CoV-2, lung, immune system, heart, clinicopathological correlation, forensic autopsy

(*Am J Forensic Med Pathol* 2021;42: 164–169)

Manuscript received August 28, 2020; accepted September 9, 2020.

From the *Department of Forensic Medicine, Tongji Medical College, Huazhong University of Science and Technology, Wuhan 430030, Hubei, China, †Hubei Chongxin Judicial Expertise Center, Wuhan 430415, Hubei, China, ‡Department of Pathology, Wuhan Jin Yin-tan Hospital, Wuhan 430023, Hubei, China, §Institute of Pathology/Department of Pathology, Tongji Hospital/Medical College, Huazhong University of Science and Technology, Wuhan 430030, Hubei, China, ||Center for Biosafety Mega-Science and Technology, Wuhan Institute of Virology Chinese Academy of Sciences, Wuhan 430071, Hubei, China, ¶Basic Medical Science and Forensic Medicine, Hangzhou Medical College, Hangzhou 310053, Zhejiang, China.

L.R., Q.L., R.W., G.W. contributed equally to this work.

Reprints: Liang Liu, MD, Tongji Medical College, Huazhong University of Science and Technology, 13 Hangkong Rd, Wuhan, Hubei 430030, China. E-mail: liuliang@mails.tjmu.edu.cn; Yiwu Zhou, MD, Tongji Medical College, Huazhong University of Science and Technology, 13 Hangkong Rd, Wuhan, Hubei 430030, China. E-mail: zhouyiwu@mails.tjmu.edu.cn; Ling Li, MD, School of Basic Medical Science and Forensic Medicine, Hangzhou Medical College, 481 Binwen Rd, Hangzhou, Zhejiang 310053, China. E-mail: ling001@aol.com.

Funding: This work was supported by the Ministry of Science and Technology of P.R. of China [2020YFC0844700 to Liang L.] and the Department of Science and Technology, Hubei Provincial People's Government [2020FCA045 to Liang L., Q. L.] and in part by Medical Research Fund of Hangzhou Medical College

Copyright © 2021 Wolters Kluwer Health, Inc. All rights reserved.

ISSN: 0195-7910/21/4202-0164

DOI: 10.1097/PAF.0000000000000644

An outbreak of COVID-19 caused by the 2019 novel coronavirus (SARS-CoV-2) emerged in Wuhan, China in December 2019 and has spread throughout China and to 200 countries/territories worldwide.¹ On March 11, the World Health Organization (WHO) declared COVID-19 outbreak a pandemic. As of August 23, 2020, the COVID-19 has killed more than 309,400 people worldwide.¹ SARS-CoV-2 infection, as is true for the related diseases, acute respiratory distress syndrome coronavirus (SARS-CoV) and Middle East Respiratory Syndrome coronavirus (MERS-CoV), predominantly affects the lower respiratory tract and manifests as pneumonia in humans.^{2–5} COVID-19 can cause a wide clinical spectrum from asymptomatic infection, mild respiratory cold-like illness, to severe pneumonia and multiorgan failure.^{6,7}

Limited forensic pathology studies have been reported based on autopsy examination. This report describes systemic autopsy findings correlated with clinicopathological features of a COVID-19 patient in Wuhan, China. We also tested different organs for SARS-CoV-2 RNA to determine the distribution of the virus in the body postmortem.

CASE REPORT

A 53-year-old woman was admitted to a designated hospital in Wuhan with dry cough, high fever and shortness of breath on January 26, 2020. She reported cold-like symptoms with dry cough and mild temperature elevation for about 7 days. She treated herself at home with Chinese herb medicine and cough syrup. Then her cough worsened and she developed chills, fatigue, chest tightness, and her body temperature rose from 38.0°C to 39.0°C in the 3 days before admission. According to the patient, she and her family members had never visited the seafood market where life animals were sold, which were thought to be the origin of this virus. All of her family member and close friends were not sick, with no fever or respiratory symptoms. She was retired and spent most of her time at home and in her community. She did not have any significant medical history. Figure 1 shows the timeline of the course of her disease.

On admission (hospital day 1, illness day 11), the patient had shortness of breath with body temperature: 38.6°C and oxygen saturation: 90%. Because of the widespread nature of COVID-19 in Wuhan by the end of January, the hospital admitted her to an isolation ward. Her admission complete blood counts revealed mild increase of neutrophils and mild decrease of lymphocytes. Her chest X-ray was remarkable for ground glass/cloud-like opacities of both lungs, consistent with an atypical/viral pneumonia (Fig. 2). Rapid IgM antibody tests for influenza A and B, parainfluenza, respiratory syncytial virus, adenovirus, mycoplasma pneumonia, chlamydia pneumonia, and legionella pneumonia were negative. Admission blood bacterial culture was reported no growth on hospital day 3.

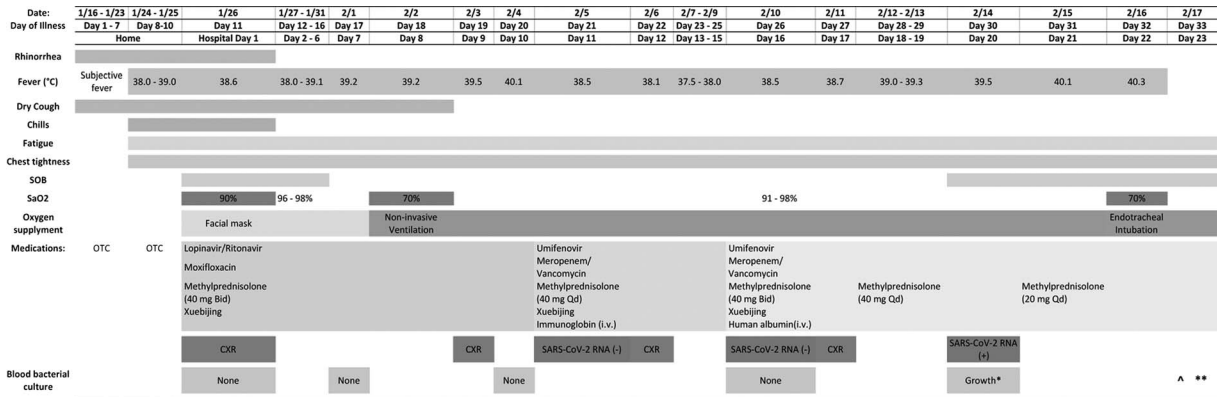


FIGURE 1. Timeline of disease course according to day of illness and day of hospitalization, January 16 to February 17, 2020. *Acinetobacter baumannii; ^: Death at 8:30 AM; **: Autopsy at 4:00 PM. SOB: shortness of breath. OTC, over-the-counter antipyretics and cough syrup.

On hospital day 10, her body temperature reached to 40.1°C. Her laboratory test results reflected severe leukocytosis with neutrophilia, lymphopenia, and thrombocytopenia (Table 1). Her chest X-ray showed persistent ground glass lesions. She was tested for SARS-CoV-2 RNA on hospital day 11 (illness day 21). Testing before this was not possible because of a significant shortage of test kits at the local hospital. Her first 2 pharyngeal swab real-time reverse transcription polymerase chain reaction (RT-PCR) tests were negative on hospital day 11 and 16 (illness days 21 and 26). On hospital day 20 (illness day 30), the SARS-CoV-2 RNA became positive. Her blood cultures on hospital days 7, 10, and 16 showed no growth, but were positive for Acinetobacter baumannii on hospital day 20 (illness day 30). Despite intensive oxygen and supportive measurements, extensive antibiotics, antiviral, and anti-inflammatory medical treatments, she developed respiratory failure with secondary bacterial infection and expired on hospital day 23 (illness day 33).

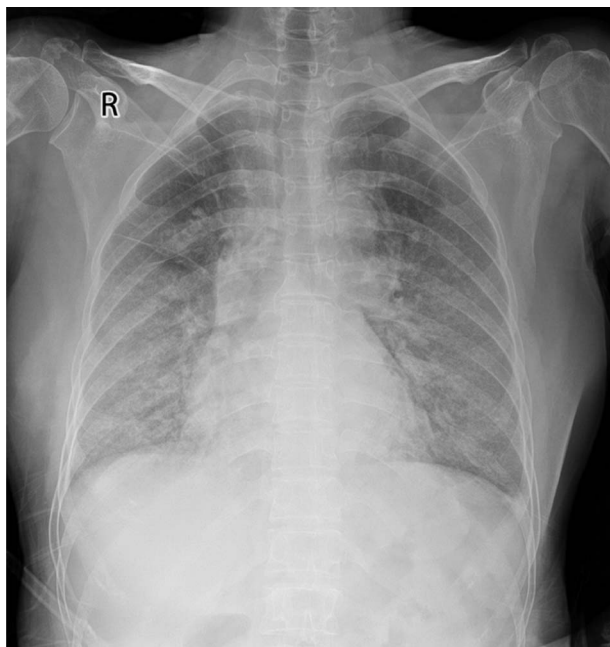


FIGURE 2. Chest x-ray image: bilateral ground-glass/cloud-like opacities, indicating atypical pneumonia on January 26, 2020 (illness day 11, hospital day 1).

MATERIALS AND METHODS

In China, the majority of hospital pathologists have never done an autopsy during their residency training and their clinical practice. Therefore, a complete autopsy was performed by forensic pathologists within 8 hours after her death. A formal consent from the next of kin was obtained prior to the autopsy. The patient's family wished that her autopsy studies would help better understand the COVID-19. The autopsy was conducted in accordance with regulations issued by the National Health Commissions of China.

Representative sections obtained from different organs were fixed in 10% buffered formalin and then paraffin-embedded, sectioned at 4 μm, and stained by routine hematoxylin and eosin. Representative lung sections were stained for by Periodic Acid-Schiff. Immunohistochemical labeling included Cytokeratin 7, CD68, CD3, and CD20 were performed on the lung tissues. CD20 and CD3 stains were conducted on spleen and lymph nodes. Small pieces of fresh lung tissue were snap fixed in 2.5% (v/v) glutaraldehyde for at least 24 hours at 4°C. Then the tissues were processed for electronic microscopy examination as published previously.⁸

RNAs were extracted from serum and fresh tissue obtained from different organs using Trizol Reagent (Invitrogen). Real-time RT-PCR detection of SARS-CoV-2 RNA was performed using a commercial diagnosis kit from Shanghai Huirui Biotechnology Co., Ltd (catalog VR-II-120), which was approved by Chinese FDA and Chinese Centers for Disease Control and Prevention. Two target genes including open reading frame 1ab (ORF1ab) and Nucleocapsid protein (N) were amplified and tested according to the manufacturer's protocol. The laboratory testing for SARS-CoV-2 was conducted following the WHO guidance.⁹

RESULTS

Figure 3A shows gross examination findings of lungs. There were thick yellowish jelly-like mucoid secretions in the bronchi and bronchiole, and an abscess with pus was seen in the right upper lobe. Hemorrhagic infarcts were present in the upper lobe and middle lobes of the right lung and diffuse consolidations were present in both lungs.

Microscopic examination of the lungs showed diffuse alveolar damage. Multiple sections of both lungs revealed diffuse hyaline membranes lining the alveolar ducts and sacs with intra-alveolar neutrophil infiltration (Fig. 3B). Multiple focal areas of both lungs showed extensive interstitial and intraalveolar proliferation of fibroblasts/myofibroblasts, with focal collagenous fibrosis (Fig. 3C), focal proliferation of pneumocytes highlighted by immunolabeling for cytokeratin (Fig. 3D). Intra-alveolar CD68 positive macrophages

TABLE 1. Clinical Laboratory Results

Measure	Reference Range	1/26/20	1/28/20	2/1/20	2/4/20	2/7/20	2/10/20	2/12/20	2/14/20	2/16/20
		Illness Day 11	Day 13	Day 17	Day 20	Day 23	Day 26	Day 28	Day 30	Day 32
		Hospital Day 1	Day 3	Day 7	Day 10	Day 13	Day 16	Day 18	Day 20	Day 22
White cell count ($\times 10^9/L$)	3.5–9.5	8.95	11.07 \uparrow	19.4 \uparrow	21.13 \uparrow	8.75	9.57 \uparrow	16.51 \uparrow	12.41 \uparrow	11.44 \uparrow
Absolute neutrophil count ($\times 10^9/L$)	1.8–6.3	8.2 \uparrow	10.46 \uparrow	18.63 \uparrow	20.53 \uparrow	8.01 \uparrow	9.13 \uparrow	15.78 \uparrow	11.82 \uparrow	9.14 \uparrow
Absolute Lymphocyte count ($\times 10^9/L$)	1.1–3.2	0.46 \downarrow	0.4 \downarrow	0.43 \downarrow	0.25 \downarrow	0.51 \downarrow	0.3 \downarrow	0.35 \downarrow	0.38 \downarrow	1.54
Absolute Monocyte count ($\times 10^9/L$)	0.1–0.6	0.28	0.19	0.32	0.32	0.2	0.13	0.35	0.2	0.09 \downarrow
Platelet count ($10^9/L$)	125–350	145	45 \downarrow	84 \downarrow	65 \downarrow	43 \downarrow	58 \downarrow	100 \downarrow	141	116 \downarrow
Hemoglobin (g/L)	115–150	118	108 \downarrow	127	112 \downarrow	93 \downarrow	95 \downarrow	106 \downarrow	102 \downarrow	94 \downarrow
Alanine aminotransferase (U/L)	7–40	24	18	55 \uparrow	39	24	32	93 \uparrow	41 \uparrow	33
Aspartate aminotransferase (U/L)	13–35	27	45 \uparrow	69 \uparrow	29	27	45 \uparrow	81 \uparrow	33	83 \uparrow
Albumin (g/L)	40–55	30.3 \downarrow	32.5 \downarrow	35.6 \downarrow	31.1 \downarrow	29.7 \downarrow	33.1 \downarrow	42.3	39.5 \downarrow	34.6 \downarrow
Total Bilirubin ($\mu\text{mol/L}$)	0–21	9.6	12.4	9.1	6.5	10.8	14.3	26.9 \uparrow	24.7 \uparrow	27.1 \uparrow
Direct Bilirubin ($\mu\text{mol/L}$)	0–8	3.8	4.2	2.1	1.6	3	2.3	5.2	8.9 \uparrow	19.9 \uparrow
Creatine kinase (U/L)	40–200	44	46	225 \uparrow	46	40	67	68	103	283 \uparrow
Blood urea nitrogen (mmol/L)	2.6–7.5	3.7	4.2	5.71	10.89 \uparrow	13.25 \uparrow	8.4 \uparrow	10.04 \uparrow	10.6 \uparrow	13.5 \uparrow
Creatinine ($\mu\text{mol/L}$)	41–73	51.4	51.9	48	47	47	35 \downarrow	47	60.8	121.8 \uparrow
Troponin I (pg/mL)	0–28	3.6					147.2 \uparrow		82.6 \uparrow	227.6 \uparrow
Prothrombin time (s)	10.5–13.5	10.6		11.1	11.6	14.3 \uparrow	11.7	13	10.1 \downarrow	
International normalized ratio (INR)	0.8–1.2	0.9		0.94	0.98	1.27 \uparrow	1.02	1.15	0.87	
Fibrinogen (g/L)	2–4	5.5 \uparrow		1.3 \downarrow	1.1 \downarrow	1.2 \downarrow	1.3 \downarrow	2.2	6.3 \uparrow	
Activated partial thromboplastin time (s)	21–37	27		26	22	24.3	19.5 \downarrow	23.4	19.1 \downarrow	

were seen in many sections (Fig. 3E). Lymphocytic infiltration was mainly CD3-positive T lymphocytes (Fig. 3F) and some CD20-positive B lymphocytes (Fig. 3G). Scattered in the lungs were also focal hemorrhagic infarcts with pulmonary arterial thrombosis. Periodic Acid-Schiff staining was negative for fungi. Electronic microscopy revealed that SARS-CoV-2-infected pneumocytes were fragmented, and single spherical viral particles ranged from 100 to 125 nm in diameter (Fig. 3H).

The brain showed acute subarachnoid hemorrhage over the right occipital region (Fig. 4A). Microscopic examination revealed fresh subarachnoid hemorrhage (Fig. 4B) and cortical venous thrombosis (Fig. 4C). The brain parenchyma showed scattered amyloid globules.

The right kidney showed 2 small cortical infarcts (Fig. 4D). Microscopic examination revealed focal ischemic infarct with renal artery thromboembolism. There were no other significant pathological changes of both kidneys. The heart weighed 270 g. There was no significant coronary artery disease. Microscopic examination of myocardium revealed focal myocyte necrosis with mild lymphocytic infiltration (Fig. 4E). The conduction system was unremarkable. The liver had no significant pathological change.

The spleen showed several subcapsular infarcts ranging from a 0.2×0.2 cm to 3.0×5.0 cm (Fig. 4F). Microscopic examination of noninfarcted area revealed severe lymphoid depletion with sparse and atrophic lymphoid nodules (Fig. 4G). There was a decrease in the number and size of CD20-stained lymphoid follicles (zones of active B cell replication) (Fig. 4H) and a decrease in CD3-positive T cell staining (Fig. 4I). The lymph nodes also had lymphoid depletion.

The thyroid gland showed focal lymphocytic thyroiditis. There was chronic inflammation of the epiglottis. The urinary

bladder had submucosal blood vessel thrombosis. The trachea, adrenals, ovary, uterus, and gastrointestinal system showed no significant pathological changes.

The real-time RT-PCR assay for SARS-CoV-2 RNA was positive in the heart, lung, kidney, spleen, liver, small intestine, and ovary, but negative in the serum, brain, and skin tissues.

DISCUSSION

The COVID-19 transmission, clinical presentation, and radiographic features are shared by previous outbreaks of SARS-CoV and MERS-CoV infections.^{2–7} This patient's illness lasted for 32 days and was hospitalized for 22 days before she died as result of COVID-19 pneumonia complicated by respiratory failure with secondary bacterial infection.

Chinese researchers isolated the SARS-CoV-2 on January 7, 2020, and then uploaded the full genetic sequence of the virus to the Global Initiative on Sharing All Influenza Data database on January 12, 2020.¹⁰ On January 16, the first RT-PCR assays for COVID-19 were distributed in Wuhan. Real-time RT-PCR of nasopharyngeal swabs was used to detect SARS-CoV-2 RNA to confirm suspected clinical diagnosis. Because of the rapid and widespread dissemination of the COVID-19 throughout China, the Chinese Centers for Disease Control and Prevention did not have enough RT-PCR test kits to test all the suspected and clinical indicated patients in a timely manner until late February. Although the patient's initial clinical presentation and her chest radiograph clinically indicated COVID-19 pneumonia, her initial 2 SARS-CoV-2 RNA tests were negative. The initial negative results on pharyngeal swabs may be explained in part by low sensitivity of pharyngeal swabs. A study of 205 hospitalized patients clinically

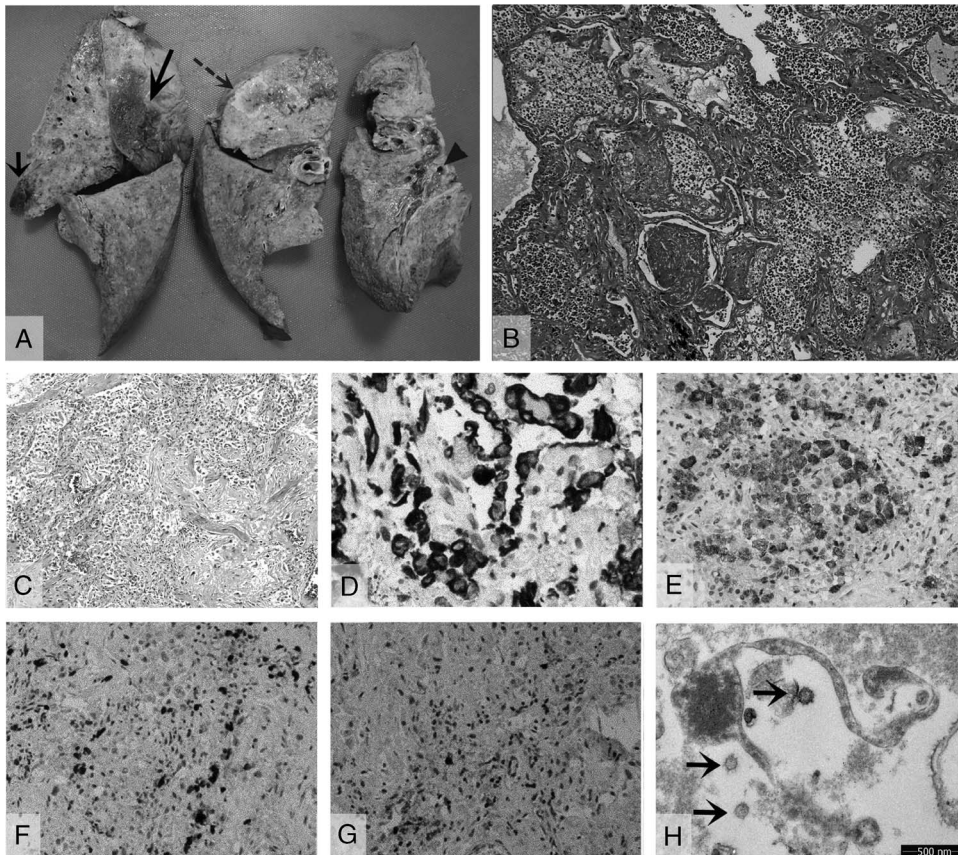


FIGURE 3. Pathological findings of the lungs. A, Gross view of the right lung with an abscess in the upper lobe (dashed arrow), a small infarct in the upper lobe (short solid arrow), a larger infarct in the middle lobe (long solid arrow), thick jelly-like mucus plug in the bronchi (arrowhead), and diffuse consolidation. B, Diffuse hyaline membrane formation with extensive intra-alveolar neutrophil infiltration (hematoxylin-eosin, original magnification, $\times 40$). C, Extensive interstitial and intra-alveolar proliferation of fibroblasts/myofibroblasts, with focal collagenous fibrosis (hematoxylin-eosin, original magnification, $\times 100$). D, Focal proliferation of Cytokeratin 7 positive pneumocytes (original magnification, $\times 200$). E, Multiple CD 68 positive macrophages (original magnification, $\times 100$). F, CD3-positive T-lymphocyte infiltrations (original magnification, $\times 40$). G, CD20-positive B-lymphocyte infiltrations (original magnification, $\times 40$). H, Fragmented pneumocyte with single spherical viral particles (arrows), electron microscope.

diagnosed with the infection revealed that pharyngeal swabs only had 32% positive rate.¹¹ With the parallel shortage of testing kits across the globe, we recommend that diagnostic evaluation and clinical treatment for COVID-19 should be guided by epidemiologic links to infected patients, clinical history, and radiographic features. Although real time RT-PCR SARS-CoV-2 RNA has been used to confirm the COVID-19, early appropriate identification and prompt isolation of clinically indicated COVID-19 patients is a key to prevent further spread of COVID-19 and to treat the patients accordingly in the setting of negative RT-PCR SARS-CoV-2 RNA.

The pathological features in the lungs of our COVID-19 patient included diffuse alveolar damage (DAD) that greatly resembles the DAD reported in SARS-CoV and MERS-CoV infections.^{12–14} Microscopically, 3 phases of DAD were observed in our patient, ranging from exudative phase with hyaline membrane formation and intra-alveolar inflammatory infiltration to fibrous proliferative/organizing-phase to early fibrotic-phase. In addition, secondary bacterial infection with pulmonary abscess was also confirmed at autopsy. Our autopsy findings demonstrate a clear clinicopathological correlation and provide the pathological evidence for the patient's respiratory failure and superimposed bacterial infection. Previous autopsy study on SARS indicated that hyaline membrane formation is typically the result of alveolar

epithelial necrosis.¹² The mechanism of DAD in COVID-19 may be similar to SARS-CoV, including a direct damage to the pneumocytes by the virus which was confirmed by our electron microscope examination with SARS-CoV-2 viral particles identified in the fragmented pneumocytes and an indirect effect mediated by subsequent immune system dysfunction,¹³ or damage by other agents, such as bacteria and oxygen toxicity. Although most of COVID-19 patients recovered from the infection, secondary bacterial infection, especially after prolonged hospitalization and oxygen ventilation, is a potentially fatal complication.

Our autopsy study also demonstrated that SARS-CoV-2 can affect several other organs, including profound adverse effect on the immune system, similar to SARS-CoV.^{15,16} Lymphopenia in circulating immune cells, severe lymphoid deletion with decreased CD20-positive B cells and CD3-positive T cells in the spleen and lymph nodes were observed in our patient. The real-time RT-PCR assay for SARS-CoV-2 RNA was positive in the spleen. The lymphopenia in COVID-19 patient presents a direct effect by the SARS-CoV-2 or in combination with corticosteroid treatment, which can also cause lymphopenia.¹⁷ Corticosteroid treatment for COVID-19 pneumonia should be closely monitored.

The pathological features of other organs in our patient included multiple infarcts with thrombosis of the lung, spleen, and

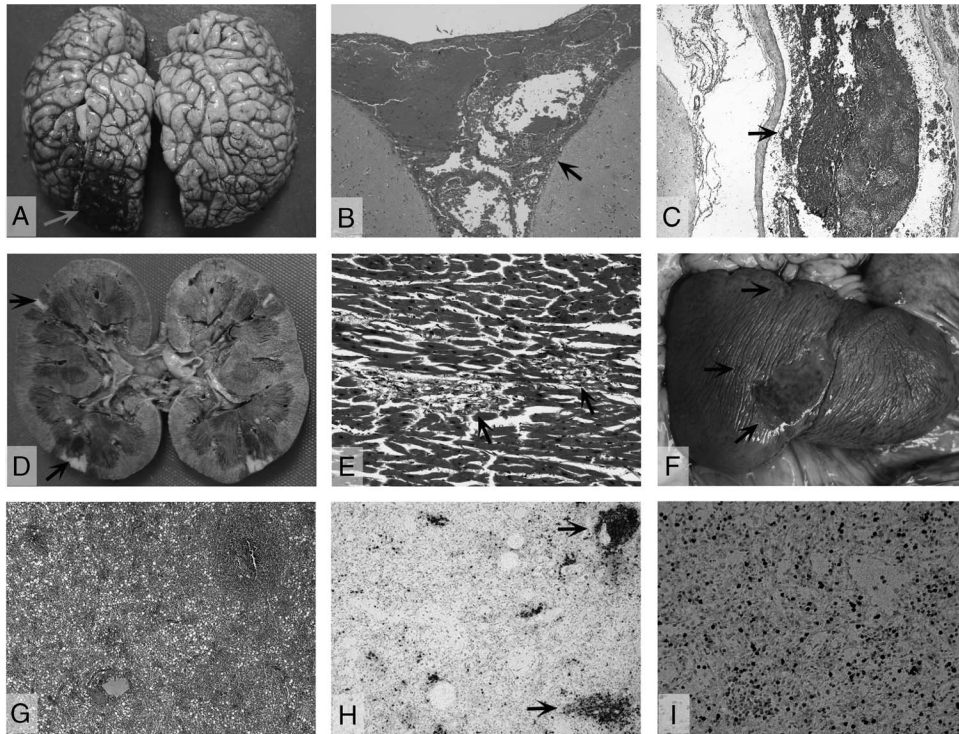


FIGURE 4. Pathological findings of other organs. A, Gross view of brain reveals focal acute subarachnoid hemorrhage over the right occipital lobe (arrow). B, Fresh subarachnoid hemorrhage (arrow). C, Cerebral cortical venous thrombosis (arrow). D, Gross view of kidney with focal ischemic infarcts (arrows). E, Focal myocyte necrosis with few lymphocytic infiltration (arrows). F, Gross view of spleen with a large infarct and several small infarcts (arrows). G, Noninfarcted areas of spleen with diffuse lymphoid depletion, hypocellular with sparse and atrophic lymphoid nodules. H, Decrease in the number and size of CD20-stained (original magnification, $\times 25$) lymphoid follicles (arrows). I, Decrease in CD3-stained T cells (original magnification $\times 100$) (hematoxylin-eosin, original magnifications: B $\times 25$, C $\times 25$, E $\times 100$, and G $\times 25$).

kidney and cerebral cortical venous thrombosis with focal subarachnoid hemorrhage. The possible mechanism of systemic thrombosis may be because of the direct viral damage to the vascular endothelial cells of the blood vessel.

Recently, one clinical study has reported cardiac involvement as a complication associated with COVID-19.¹⁸ A postmortem cardiac biopsy study in a COVID-19 patient described focal myocardial interstitial inflammatory cells.¹⁶ In our patient, the myocardium revealed focal myocyte necrosis with mild lymphocytic infiltration consistent with focal viral myocarditis. The real-time RT-PCR assay for SARS-CoV-2 RNA was also positive in the myocardial tissue, which provides pathological evidence of cardiac injury by COVID-19.

Remarkably, SARS CoV-2 RNA was detected in the heart, lung, spleen, liver, kidney, small intestine, and ovary. Although the liver showed no significant pathological change in our patient, a recent case report indicated hepatitis associated with COVID-19.¹⁹ The detection of SARS CoV-2 RAN in multiple organs postmortem may reflect a process of replication and dissemination of the virus through the blood or the lymphatic system from the respiratory tract,¹⁸ and further study is needed in more autopsy cases to determine the nature of damage and target organs/cells by COVID-19.

It has been a great challenge for pathologists to study diseases because of the dramatic decline in hospital autopsies in China. The main reasons for very few hospital autopsies include an emphasis of surgical pathology in clinical diagnosis and Chinese cultural opposition to autopsy. To the best of our knowledge, the majority of Chinese hospitals have no autopsy room, and more than 90% hospital pathologists have never performed any autopsies. Almost all the autopsies performed in China are cases related

to medicolegal purposes, which are conducted by forensic pathologists. Therefore, forensic pathologists are the only well-trained and well-skilled pathologists who are able to conduct systemic autopsy in China. Forensic autopsy has been proved to be the criterion standard to identify the cause of death in individuals who die suddenly and unexpectedly.²⁰ However, our current case also demonstrates the important role of forensic pathologists in the study of infectious disease because of the lack of autopsy skills by hospital pathologists in China. This autopsy study has provided invaluable clinicopathological features of the COVID-19 to better understand the pathogenesis of this novel virus and to help in the clinical treatment.

ACKNOWLEDGMENTS

Supported by the Hubei Science and Technology Plan (2020FCA045 to Liang Liu and Qian Liu), Ministry of Science and Technology of P.R. China Plan (2020YFC0844700 to Liang Liu), and in part by the Medical Research Fund of Hangzhou Medical College. The researches confirm their independent from the founders and sponsors.

REFERENCES

1. World Health Organization. Coronavirus disease (COVID-2019): Weekly Epidemiological Update. Available at: https://www.who.int/docs/default-source/coronaviruse/situation-reports/20200824-weekly-epi-update.pdf?sfvrsn=806986d1_4.
2. Peeri NC, Shrestha N, Rahman MS, et al. The SARS, MERS and novel coronavirus (COVID-19) epidemics, the newest and biggest global health

- threats: what lessons have we learned? *Int J Epidemiol.* 2020;49:717–726. doi:10.1093/ije/dyaa033.
3. Hui DS, Wong PC, Wang C. SARS: clinical features and diagnosis. *Respirology.* 2003;8 Suppl(Suppl 1, 4):S20.
 4. Guan WJ, Ni ZY, Hu Y, et al. Clinical characteristics of coronavirus disease 2019 in China. *N Engl J Med.* 2020;382:1708–1720. doi:10.1056/NEJMoa2002032.
 5. Sohrabi C, Alsafi Z, O'Neill N, et al. World Health Organization declares global emergency: a review of the 2019 novel coronavirus (COVID-19). *Int J Surg.* 2020;76:71–76.
 6. Chen N, Zhou M, Dong X, et al. Epidemiological and clinical characteristics of 99 cases of 2019 novel coronavirus pneumonia in Wuhan, China: a descriptive study. *Lancet.* 2020;395(10223):507–513.
 7. Wang D, Hu B, Hu C, et al. Clinical characteristics of 138 hospitalized patients with 2019 novel coronavirus-infected pneumonia in Wuhan. *China JAMA.* 2020;323:1061–1069. doi:10.1001/jama.2020.1585.
 8. Liu J, Xu M, Tang B, et al. Single-particle tracking reveals the sequential entry process of the Bunyavirus severe fever with thrombocytopenia syndrome virus. *Small.* 2019;15(6):e1803788.
 9. World Health Organization. Laboratory testing for 2019 novel coronavirus (2019-nCoV) in suspected human cases. 2020. Available at: <https://www.who.int/publications-detail/laboratory-testing-for-2019-novel-coronavirus-in-suspected-human-cases-20200117>.
 10. World Health Organization. *Report of the WHO-China Joint Mission on Coronavirus Disease.* 2019; (COVID-19). 2020. Available at: <https://www.who.int/docs/default-source/coronaviruse/who-china-joint-mission-on-covid-19-final-report.pdf>.
 11. Wang W, Xu Y, Gao R, et al. Detection of SARS-CoV-2 in different types of clinical specimens. *JAMA.* 2020. doi:10.1001/jama.2020.3786.
 12. Lee N, Hui D, Wu A, et al. A major outbreak of severe acute respiratory syndrome in Hong Kong. *N Engl J Med.* 2003;348(20):1986–1994.
 13. Arabi YM, Balkhy HH, Hayden FG, et al. Middle East respiratory syndrome. *N Engl J Med.* 2017;376(6):584–594.
 14. Franks TJ, Chong PY, Chui P, et al. Lung pathology of severe acute respiratory syndrome (SARS): a study of 8 autopsy cases from Singapore. *Hum Pathol.* 2003;34(8):743–748.
 15. Guo Y, Korteweg C, McNutt MA, et al. Pathogenetic mechanisms of severe acute respiratory syndrome. *Virus Res.* 2008;133(1):4–12.
 16. Xu Z, Shi L, Wang Y, et al. Pathological findings of COVID-19 associated with acute respiratory distress syndrome. *Lancet Respir Med.* 2020;8:420–422. doi:10.1016/S2213-2600(20)30076-X.
 17. Ng DL, Al Hosani F, Keating MK, et al. Clinicopathologic, immunohistochemical, and ultrastructural findings of a fatal case of Middle East respiratory syndrome coronavirus infection in the United Arab Emirates, April 2014. *Am J Pathol.* 2016;186(3):652–658.
 18. Inciardi RM, Lupi L, Zaccone G, et al. Cardiac involvement in a patient with coronavirus disease 2019 (COVID-19). *JAMA Cardiol.* 2020;5:819–824. doi:10.1001/jamacardio.2020.1096.
 19. Lagana SM, De Michele S, Lee MJ, et al. COVID-19 associated hepatitis complicating recent living donor liver transplantation. *Arch Pathol Lab Med.* 2020;144:929–932. doi:10.5858/arpa.2020-0186-SA.
 20. Li L, Burke A, He J, et al. Sudden unexpected death due to inflammatory myofibroblastic tumor of the heart: a case report and review of the literature. *Int J Leg Med.* 2011;125(1):81–85.